ELSEVIER

Journal of Nuclear Materials 274 (1999) 34–39

journal of nuclear materials

www.elsevier.nl/locate/jnucmat

Modelling, manufacturing and thermomechanical characterization of spinel–uranium dioxide composite fuels

I. Munoz-Viallard *, M. Bauer, J.-M. Bonnerot

Département d'Etude des Combustibles, Commissariat à l'Energie Atomique (CEA), CEA/Cadarache, DRN/DEC/SPU Bat. 315, F-13108 Saint-Paul-Lez-Durance, France

Abstract

The present paper describes laboratory studies performed on composite materials made of a spinel inert matrix in which uranium dioxide particles are dispersed. This study aims to improve the lifetime of the standard nuclear fuel. The work involves the modelling of the thermomechanical in-pile behavior of these materials, manufacturing tests and out-of-pile characterizations. The influence of some physical characteristics such as the particle size and the nature of the matrix–particle interface inside the composite is analysed. The results show a very good out-of-pile mechanical behavior of the composite material, especially a high ability to deform and excellent thermal gradient resistance.

1. Introduction

In order to increase the fuel burn-up (currently 47 GWd tU^{-1} [1]) in French pressurized water reactors (PWR), while keeping the same safety level, a new fuel concept is currently studied: it consists of a composite material.

This composite fuel is made of a ceramic spinel matrix, $MgAl_2O_4$, in which uranium dioxide particles are dispersed. The matrix plays the role of a physical barrier against the fission product release and allows increases in the total thermal conductivity of the fuel. This in turn, lowers the pellet centre temperature and, as a consequence, the thermal gradient between the centre and the periphery of the pellet. The loading level of particles is 40 vol.% which represents the best compromise between the economical cost of the corresponding enrichment of UO_2 in ^{235}U and the efficiency of the barrier for the fission product release. On the basis of neutronic calculations, this loading level induces a 100 μm minimal particule size in order to avoid matrix damage under irradiation due to fission product recoil. In this work, the size of the macrospheres will vary up to 300 μm.

First of all, a model is developed to predict the thermal and mechanical in-pile behavior of $MgAl_2O_4$–UO_2 composite materials. It allows evaluation of the influence of the structural characteristics of the composite (nature of the matrix–macrosphere interface, particle size) on the temperature distribution between the centerline and the pellet surface, and on resultant thermal stresses, under irradiation. From the model results, three types of composite materials are selected and studied. They differ in the nature of their matrix–particle interface and in the structure of their macrospheres.

2. Modelling of the composite material in-pile behavior

2.1. Model geometry

A 2D calculation is performed by means of a finite element method implemented into the CASTEM 2000 code, in order to evaluate the thermomechanical in-pile behavior of composite fuels consisting of an inert matrix in which specific size macrospheres are dispersed.

This model is required to define a specific calculation mesh that considers uniform distribution of identical disks as particles dispersed in the inert matrix, and the possibility of providing a gap between the matrix and the particle. The macrospheres are then simulated by an arrangement of identical cylindrical particles, which is in

* Corresponding author. Fax: +33-4 42 25 47 17; e-mail: Isabelle.munoz-viallard@cea.fr

0022-3115/99/$ – see front matter
PII: S0022-3115(99)00040-9

the state of plane strain. A corrective factor takes into account the spherical shape of the particle. The arrangement is such that the volume fraction of macrospheres is 40%. The size of the particles can be varied and consequently the number of macrospheres is adjusted in order to keep the same 'volume' fraction of particles. The mesh represents the plane section of the pellet and only a sectional part of the symmetric matrix is analysed.

For the simulation, the specific power emitted by the macrospheres is adjusted to develop a total linear power density equal to that of a PWR fuel in standard operating conditions.

2.2. Collected data and results

The calculated data are:

- radial temperature profile within the matrix and the macrospheres (>100 μm in diameter),
- associated radial and tangential mechanical stresses.

A large number of simulations show that:

- radial temperature profile in the pellet is parabolic, whatever the parameters are;
- radial thermal gradient between the centre and the periphery of the pellet is equal to approximately 7.5×10^{-2} K m^{-1}, which is much less than the one existing in the standard PWR fuel (approximately 16.2×10^{-2} K m^{-1});
- higher tensile stresses are located in the matrix and at the periphery of the pellet, because of the high thermal gradient that exists between the centre and the surface of the pellet;
- stresses are higher in the matrix than in the fissile macrospheres;
- stresses are minimized for small particle sizes [2];
- stresses are partially released by the presence of a gap at the matrix–macrosphere interface.

However, the intensity of the stresses in the matrix is higher than the fracture strength of $MgAl_2O_4$, leading to probable microcracking of the matrix. Even if crack initiation cannot be avoided, the composite microstructure can be designed to control crack propagation within the pellet. Moreover, the integrity of the pellet can be preserved. This in turn can lead to a reduction of the clad–pellet interaction and a better containment of the fission products.

2.3. Choice of specific microstructures

On the basis of these results, three types of structures have been retained and studied:

- a reference material (A), without major microstructural flaws (without microcracks and with a strong matrix–particle interface), containing particles of 120 μm in diameter and as spherical as possible;
- a material with microcracks inside the particles (material B);
- a material containing weak interfaces between the spinel matrix and the 120 μm macrospheres (material C): in our case, a definite gap is provided in order to release stresses (these stresses reach the highest values at the interface).

Material (A) is likely to be the best regarding the overall thermal conductivity, minimizing the thermal gradient between the centre and the periphery of the pellet, and as a consequence, minimizing the thermal stress intensity during irradiation.

When loading material (B), microcracking can appear due to the effect of the stress field created around the particles. This increases elastic energy by absorption and thus contributes to a fracture energy increase.

Material (C) allows a stress decrease at the interface between the spinel matrix and the macrospheres. The voids created around the fissile particles can also provide an expansion volume area for the fission products.

3. Pellet manufacturing

The pellets are processed by applying a classical powder metallurgy route. The macrospheres are first produced from the process as described in Fig. 1.

The fissile material powder UO_2 (spray dried UO_2 from Cogema [3]) is compacted to approximately

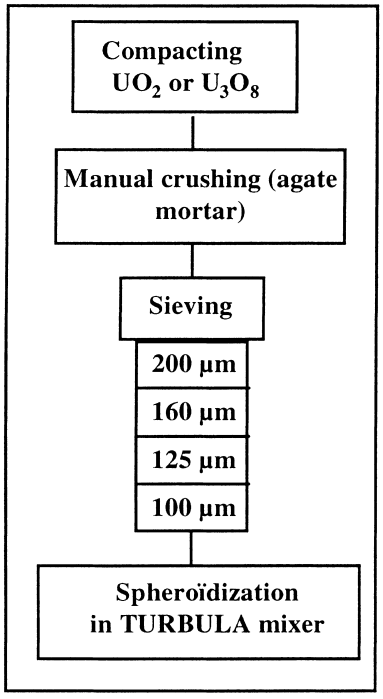

Fig. 1. Macrospheres manufacturing process.

100 MPa, granulated, and sieved to obtain granules of 125–160 μm in size (standard case). Then the granules are eroded by mechanical mixing (rotative mixing media) in order to optimise the shape of the macrospheres. For the reference material (A), the particles are annealed at about 1523 K, for consolidation treatment. For material (B), the macrospheres are not consolidated in order to enhance microcracking.

The macrospheres are then homogeneously mixed with the spinel powder (Baïkowsky). The mixing is then compacted in a double effect die, to a pressure of 300 MPa. Finally sintering of the green pellets is performed in a hydrogen atmosphere containing 2 vol% of water, at 1923 K for 1 h. This method of sintering produces pellets of high final densities (>94.5% of the theoretical density in both cases) on condition that the spinel powder starts its densification after the UO_2 powder does, in order to accommodate the stresses [3].

A gap can be created around the macrosphere from the original method [4]. It consists of using U_3O_8 (CEA) as basic powder for macrospheres manufacturing. The volumic shrinkage induced by the chemical transformation of U_3O_8 (orthorhombic) into UO_2 (cubic) under a reducing atmosphere produces a gap around each

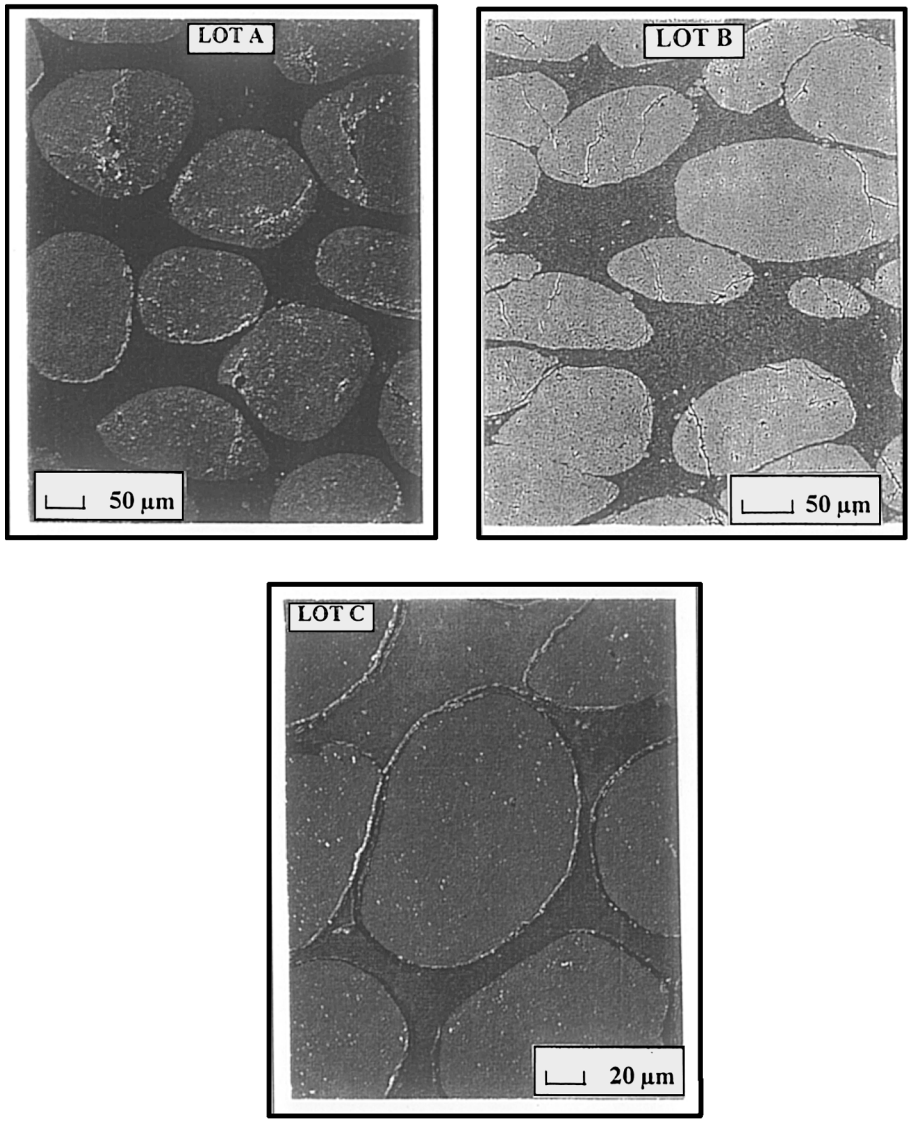

Fig. 2. Optical micrographs of the three types of composite materials studied. (a) Cohesive matrix (spinel)–macrosphere (UO_2) interface (material A). (b) Microcracking of the UO_2 particles (material B). (c) Weak matrix–macrosphere interface (material C) – definite gap between spinel (matrix) and UO_2.

second-phase particle. In this case, the heat treatment is not necessary.

The optical micrographs show a uniform distribution of the macrospheres within the composite materials. The matrix–particle interface is cohesive (Fig. 2(a)) in material A and a gap is really created in material C (Fig. 2(c)).

The 19 vol.% lattice shrinkage observed induced a 1–2 μm final gap around the fissile particles. In material B, microcracking of the particles (Fig. 2(b)) and a strong matrix–particle interface are observed, and the particles are no longer spherical.

4. Thermomechanical behavior

The mechanical properties of these composites are first determined at room temperature and then compared with the corresponding pure materials of similar density. Next a specific device is developed in order to reproduce the stresses induced under irradiation.

From cylindrical large diameter pellets, thin discs are machined for biaxial bending and thermal gradient resistance tests. The physical property measurements are then representative of PWR conditions, the geometry of the sample being close to standard fuel.

4.1. Procedure

Biaxial bending strength testing is less sensitive to edge-effects than are classical methods such as traction, 3 or 4 point bending tests [5–8]. Our tests were carried out using the ball-on-3 balls method. The sample is a thin disc of 1 mm in thickness (diameter/thickness >10) supported by three balls on the periphery of the sample. The load is applied via another ball, centred on the upper side of the disc.

The maximum radial and tangential stresses ($\sigma_{\max.}$) are located in the centre of the specimen where they are equal. They are given by [8]

$$\sigma_{\max.} = \frac{3 \cdot F \cdot (1+\nu)}{4 \cdot \pi \cdot d^2} \times \left\{ 1 + 2 \cdot \ln\left(\frac{r_s}{r_f}\right) + \frac{(1-\nu) \cdot r_s^2}{(1+\nu) \cdot R^2} \left[1 - \left(\frac{r_f^2}{2 r_s^2} \right) \right] \right\}, \quad (1)$$

where F is the load, d the disc thickness, r_s the radius of the circle of support points, R the radius of the disc, ν the Poisson's ratio and r_f the radius of a fictitious region of uniform loading at the center of the disc. In our case, as estimated from the Hertz elastic contact stress equation between a plate and a ball, r_c, the contact radius of the loading ball with the specimen, is very small compared to d. Here, $r_f = 0.325d$ [5].

About 10 samples were tested for each type of material.

Toughness K_{1c} is evaluated from the single-edge notch-beam method, under uniaxial 3-point bending. It is given by [9]

$$K_{1c} = \sigma_{\max.} \cdot Y \cdot \sqrt{a_c}, \quad (2)$$

where $\sigma_{\max.}$ is the maximal stress calculated from the 3-point bending equations

$$\sigma_{\max.} = \frac{3 \cdot F \cdot L}{2 \cdot l \cdot h^2}, \quad (3)$$

where l and h are the width and the height of the sample, respectively, and L is the distance between the two support bars, a_c is a constant relavent to the dimension of the sample notch and Y is given by

$$Y = 1.99 - 2.47 \cdot x + 12.97 \cdot x^2 - 23.17 \cdot x^3 + 24.80 \cdot x^4, \quad (4)$$

where

$$x = \frac{a_c}{h}. \quad (5)$$

The tests are carried out on a 20 kN press, which allows very slow deformation (down to 5 μm min^{-1}). The measured strain is corrected to take into account the stiffness of the support.

Thermal shock resistance tests were carried out in an image furnace and aimed to reproduce the stresses induced within the pellet under irradiation. The corresponding device is described in Fig. 3.

The sample is located on a water-cooled specimen holder. Heat is produced by two high power halogen bulbs. Two elliptic reflectors focus light in the centre of the sample. The temperature is measured with two thermocouples, one is in the centre of the disc, the other on the periphery. A thermal gradient is then obtained between the centre and the periphery of the sample. It can reach 75 K mm^{-1} depending on the nature of the material, which is similar to those occurring in PWR conditions for this kind of material. Furthermore, it leads to realistic thermal stresses as it was shown on tests on other composite materials [10]. An inert local atmosphere is created around the specimen in order to avoid oxidation of UO_2 during the test. The different

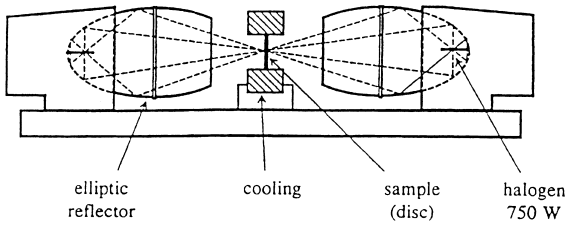

Fig. 3. Unit used for thermal gradient resistance test.

specimens are submitted to increasing heat power until they crack and/or break.

4.2. Results

Characteristic stress–deformation curves are presented in Fig. 4. The pure materials show a brittle behavior and break at the end of the test.

However, it is striking to observe that the composite material behaves differently:

- the curve initially is linear;
- the second part of the curve shows steps, each of them corresponding to the propagation of a crack from the centre to the periphery of the sample;
- after a total deformation of 60 μm, the sample is cracked, but not broken.

The maximum strength values, obtained using Eq. (1), are inferior to that of the pure materials, whatever the type of the composite material and whatever the size of the macrospheres are (Tables 1 and 2). This was expected due to the large size of the macrospheres.

Table 1 shows that a 'weak' interface leads to a decrease in maximum strength. The lack of contact between the matrix and the particles makes the composite behaving like a porous material with pores of 120 μm in diameter.

Table 2 shows that the maximum strength decreases when the particle size increases according to the literature [11] and so does the toughness, due to fundamental crack propagation mechanisms [12–16]. All the composites show the same stress/strain behavior. However the materials including large size particles ($\geqslant$200 μm) lead to fracture as opposed to other composite materials.

The best material regarding toughness is B, which presents a stronger interface and microcracked particles. Toughness is equal or higher (up to 80% higher) than the standard fuel material in cases A and B, where the matrix–particle interface is cohesive. When the interface is decohesive (C case), the material behaves in a porous manner.

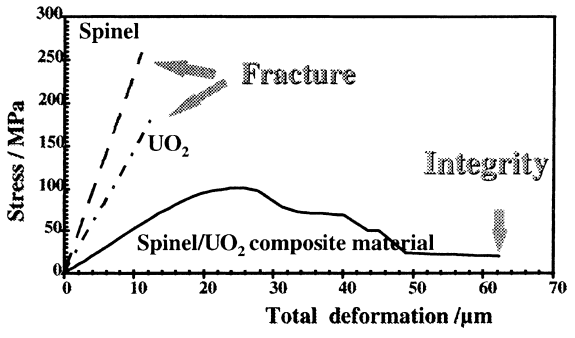

Fig. 4. Stress versus total deformation of spinel, UO_2 and spinel–UO_2 composite materials (material A, $d = 1$ mm).

Table 1
Influence of the matrix–macrosphere interface (macrospheres of 120 μm in size) on strength and toughness

	$\sigma_{max.}$ (MPa)	Aspect	K_{1C} (MPa m$^{1/2}$)
$MgAl_2O_4$	223 ± 3	Broken	2.8 ± 0.1
UO_2	180 ± 9	Broken	1.2 ± 0.1
A	101 ± 10	Cracked	1.4 ± 0.1
B	108 ± 9	Cracked	2.2 ± 0.1
C	61 ± 6	Cracked	0.6 ± 0.1

Table 2
Influence of the size of the macrospheres (material A) on strength and toughness

Size of macrospheres μm	$\sigma_{max.}$ (MPa)	Aspect	K_{1C} (MPa m$^{1/2}$)
100	102 ± 8	cracked	1.5 ± 0.1
120	101 ± 10	cracked	1.4 ± 0.1
160	82 ± 16	cracked	1.2 ± 0.1
200	78 ± 7	broken	1.2 ± 0.1

Thermal shock resistance tests show excellent behavior of the composites ($\Delta T/\Delta L > 75$ K mm^{-1}) compared with the UO_2 material ($\Delta T/\Delta L = 25$ K mm^{-1}). As opposed to the standard fuel, the composite samples keep their integrity under thermal stresses similar to the ones induced under irradiation. Cracks remain stable even with higher heating.

5. Conclusion and outlook

A very significant improvement of the thermomechanical properties of the fuel pellet is obtained with the composite structures: their ability to deform under stresses is much higher than UO_2, and excellent thermal shock resistance is observed, without any fracture of the sample. This forecasts a better behavior of the composite fuel pellets during the first power increase in reactor, in terms of pellet cladding interaction (PCI). The samples keep their integrity, provided the size of macrospheres is less than 200 μm. Therefore, the apparent diameter of the composite pellet under irradiation will be reduced compared to standard UO_2 fuel. This could be favorable for a reduction of PCI during irradiation (i.e., no relocation).

In the future, the creep behavior of these materials will be studied in order to confirm the potential benefit provided by this new concept in terms of PCI. Moreover, irradiation experiments must be carried out to corroborate these results.

An analytical irradiation, named THERMET is currently underway, in order to study the in-pile thermal behavior of such composite materials. Post irradiation experiments are taking place. Results should be avail-

able in the near future. The ability to retain the fission gas release will be evaluated during other irradiation experiments.

It is anticipated that this concept of composite materials may be applied to the recycling of minor actinides in PWR. In such a case, UO_2 would be replaced by minor actinides and the inert matrix would be efficient for fission product retention during transmutation.

References

[1] S. Roudier, R. Berama, in: Proceedings of the Nuclear fuel in France: on ever changing world most recent safety concerns of DSIN specialist meeting on Nuclear fuel and control rod, Madrid, 5–7 Nov. 1996.
[2] J. Selsing, J. Am. Ceram. Soc. 44 (1961) 419.
[3] I. Viallard, PhD thesis INSA Lyon, France, 1996, p. 227.
[4] I. Viallard, J.M. Bonnerot, J.P. Fleury, French Patent CEA No. 96 01500.
[5] G. De With, H.M. Wagemans, J. Am. Ceram. Soc. 72 (8) (1989) 1538.
[6] F.F. Vitman, V.P. Pukh, Zavod. Lab. 29 (7) (1963) 863.
[7] A.F. Kirstein, R.M. Woolley, J. Res. Nat. Bur. Stand. 71C (1) (1967) 1.
[8] S. Timoshenko, S. Woinowsky-Krieger, Theory of Plates and Shells, 2nd Ed., Mc Graw-Hill Kogakusha, New York, 1959.
[9] G.R. Irwin, J. Appl. Mech. 24 (1957) 361.
[10] D. Gosset, G.M. Decroix, B. Kryger, in: Proceedings of the 11th International Symposium Boron, Borides and Related Compounds, Tsukuba, 1993, J. Jpn. Series 10 (1994) 216–219.
[11] R.L. Fullman, Trans. Adv. Mech. 193 (3) (1953) 447.
[12] K.T. Faber, T. Iwagoshi, A. Ghosh, J. Am. Ceram. Soc. 71 (9) (1988) C399.
[13] R.W. Rice, Ceram. Eng. Sci. Proc. 11 (7/8) (1990) 667.
[14] F.F. Lange, Philos. Mag. 1327 (179) (1970) 983.
[15] M. Taya, S. Hayashi, A.S. Kobayashi, H.S. Yoon, J. Am. Ceram. Soc. 73 (5) (1990) 1382.
[16] P.F. Becher, J. Am. Ceram. Soc. 74 (20) (1991) 255.